Microchimica Acta (2021) 188:243
https://doi.org/10.1007/s00604-021-04882-2

ORIGINAL PAPER

Enzymatic photoelectrochemical bioassay based on hierarchical CdS/NiO heterojunction for glucose determination

Hui-Yu Zou[1,2] · Fen-Ying Kong[1,2] · Xin-Yang Lu[1,2] · Meng-Jiao Lu[2,3] · Yuan-Cheng Zhu[2,4] · Rui Ban[3] · Wei-Wei Zhao[2] · Wei Wang[1,2]

Received: 5 April 2021 / Accepted: 31 May 2021
© The Author(s), under exclusive licence to Springer-Verlag GmbH Austria, part of Springer Nature 2021

Abstract

The design and development of a 3D hierarchical CdS/NiO heterojunction and its application in a self-powered cathodic photoelectrochemical (PEC) bioanalysis is introduced. Specifically, NiO nanoflakes (NFs) were in situ formed on carbon fibers via a facile liquid-phase deposition method followed by an annealing step and subsequent integration with CdS quantum dots (QDs). The glucose oxidase (GOx) was then coated on the photocathode to allow the determination of glucose. Under 5 W 410 nm LED light and at a working voltage of 0.0 V (vs. Ag/AgCl), this method can assay glucose concentrations down to 1.77×10^{-9} M. The linear range was 5×10^{-7} M to 1×10^{-3} M, and the relative standard deviation (RSD) was below 5%. The photocathodic biosensor achieved target detection with high sensitivity and selectivity. This work is expected to stimulate more passion in the development of innovative hierarchical heterostructures for advanced self-powered photocathodic bioanalysis.

Keywords Photoelectrochemical biosensor · Glucose determination · Self-powered photocathode · CdS · NiO · Hierarchical heterojunction

Introduction

Photoelectrochemical (PEC) bioanalysis is a novel technology for addressing biomolecules based on the integration between photoactive materials and biometric events. Due to its satisfactory features such as high sensitivity, low background, and easy miniaturization, PEC bioassay has developed more vigorously in recent years [1–4]. The self-powered biosensors without the external power sources have attracted extensive research interest because of the difficulty in replacing batteries in devices, for example, implanted biomedical monitoring or treatment systems [5–9]. Using semiconductors to in situ convert the light into electricity, self-powered PEC bioanalytical platforms have received large amounts of attention [10–13]. Especially, the photocathodes possessed better anti-interference capacity compared to the photoanodes [14–18]. Hence, the self-powered photocathodic biosensor becomes a more desirable choice.

One of the important keys to construct such a sensor is the development of high-performance photocathode [19–21]. The hinge to enhance the photoelectric activity of photocathode is to design a more suitable photoelectric active material. Heterojunctions are hierarchical structures composed of two or more building blocks such as crystals, nanowires, nanorods, and nanosheets [22–25]. Compared to single-component materials, hierarchical heterojunctions have many unique merits, such as specific electronic responses due to their abundant active sites, larger specific surface area, and efficient electronic transmission path [26–28]. Benefiting from these advantages, proper design and construction of hierarchical heterojunction-based photocathode represent a new

✉ Fen-Ying Kong
kongfy@ycit.edu.cn

✉ Yuan-Cheng Zhu
yczhu@nju.edu.cn

✉ Wei Wang
wangw@ycit.edu.cn

1 School of Chemistry and Chemical Engineering, Yancheng Institute of Technology, Yancheng 224051, China

2 State Key Laboratory of Analytical Chemistry for Life Science, School of Chemistry and Chemical Engineering, Nanjing University, Nanjing 210023, China

3 School of Chemical Engineering, Guizhou Minzu University, Guiyang 550025, China

4 State Key Laboratory of Pharmaceutical Biotechnology, School of Life Science, Nanjing University, Nanjing 210023, China

Published online: 06 July 2021

research direction for advanced PEC bioanalysis. Recently, the potential of hierarchical heterojunctions in PEC bioanalysis has been revealed [29–32].

Glucose is one of the most essential compounds for vital movement. Not only participate in the energy supply of life activities, but also an important marker of various diseases such as diabetes and glucose metabolism disorders [33]. Up to now, various of glucose detection methods have been reported, including high-performance liquid chromatography (HPLC), gas chromatography (GC), copper iodometry, and capillary zone electrophoresis (CZE) [34–37]. These methods often rely on expensive equipment, require delicate manual manipulation, and showed universality. Thus, it attracted many researchers to developing convenient, low-cost, and high specificity glucose detection methods.

In this study, to develop a more efficient and accurate method for the detection of glucose, we presented a self-powered photocathodic biosensor on the basis of a 3D hierarchical CdS/NiO heterojunction. Among various p-type semiconductor materials, NiO stands out by virtue of its low fabrication cost and high accessibility via simple methods. To overcome its issue of wide band gap (ca. 3.6–4.0 eV), an n-type thioglycolic acid (TGA)–capped CdS quantum dots (QDs) with a narrow band gap (ca. 2.42 eV) was selected to sensitize the NiO. As illustrated in Scheme 1, NiO nanoflakes (NFs) were in situ formed on a carbon fiber network (CFN) via a facile liquid-phase deposition method and an annealing step. Next, a stable coordination compound of CdS QDs/NiO NFs was formed by integrating the COOH groups on CdS QDs surface with Ni atom. Finally, glucose oxidase (GOx) was immobilized on the surface of CdS QDs/NiO NFs/CFN to obtain a GOx/CdS QDs/NiO NFs/CFN biosensor. (More details are given in supplementary data.) Exemplified by such a GOx/CdS QDs/NiO NFs system, the self-powered photocathodic biosensor was successfully applied for glucose detection with high sensitivity and selectivity. This work features the development of 3D hierarchical CdS/NiO heterojunction and its application for a high-performance self-powered photocathodic biosensor towards enzymatic detection of glucose as a model target. We envision it could inspire more passion in the innovation of novel hierarchical heterostructures and its application in self-powered photocathodic bioanalysis.

Experimental section

Synthesis of the TGA-stabilized CdS QDs

The utilized TGA-CdS QDs were synthesized and refer to the former report with a slight variation [38]. First, 100 mL 0.01 M $CdCl_2$ and 500 μL TGA were added into a 200 mL three-necked flask, and then adjusted the mixed solution to the expected pH 11 by 1 M NaOH, heated to 110°C and stirred continuously for 30 min. Next, added 10 mL 0.1 M Na_2S into the three-necked flask and refluxed for 4 h. All the experiments were conducted under the N_2 bubbled throughout the solution.

Preparation of 3D CdS QDs/NiO NFs/CFN electrode

First, cut the CFN into 0.7 cm×3.3 cm slices and then plasma for 5 min to enhance surface hydrophilicity. Next, the CFNs were dipped into a beaker containing liquid precursors composed of 14 mL 0.03 M $NiCl_2{\cdot}6H_2O$, 14 mL 0.09 M HF, and 300 μL 13 M $NH_3{\cdot}H_2O$, and reaction at 60 °C for 2.5 h. Then, the CFNs were washed with ultrapure water and dried at room temperature and annealed under 400 °C for 2 h, obtained NiO NFs/CFN. Next, the prepared NiO NFs/CFN electrode was dipped into TGA-CdS QDs solution for 2 h, followed with

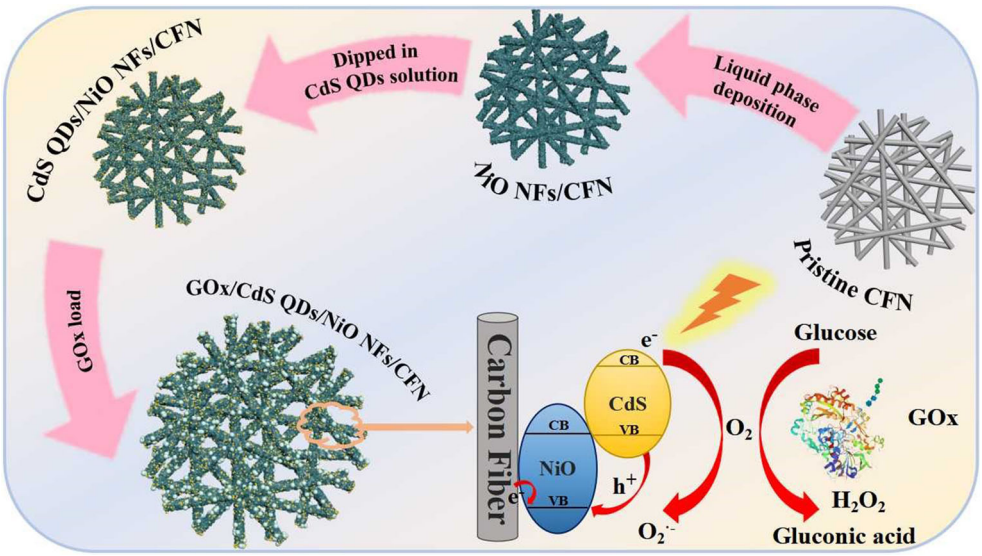

Scheme 1 Schematic diagram of CdS QDs/NiO NFs/CFN electrode assembly process and electron transfer under light irradiation

sufficient washing to remove non-bonded CdS QDs on the surface.

Cathodic photoelectric biosensor development

To incorporate with the GOx, the CdS QDs/NiO NFs/CFN was immersed in the mixture solution consisting of 20 mg mL^{-1} EDC and 10 mg mL^{-1} NHS (volume ratio 1:1) at room temperature for 1 h, then washed by washing buffer slightly and dried. Next, 25 μL 1112.5 U mL^{-1} GOx was dropped onto the electrode surface and reacted at 4 °C overnight. Finally, rinsed with washing buffer to remove the nonspecific adsorbed enzyme. For the photoelectrochemical test, the obtained GOx/CdS QDs/NiO NFs/CFN electrode was immersed into 7 mL 0.1 M Tris-HCl buffer (pH 7.0) with 10 μL different concentration glucose or complex sample, and recorded the photocurrent after incubated at 37 °C for 10 min.

Results and discussion

Characterization

The gradual change process of electrode surface structure morphology was recorded by scanning electron microscopy (SEM). From Fig. 1, we can see that the microstructure of CFN had changed significantly with the sequential assemble of NiO NFs and CdS QDs. According to Fig. 1a and inset, pristine CFN appeared an interlaced 3D meshwork structure and the corresponding magnified part had coarse textures on the surface. These textures were conductive to the subsequent formation of NiO NFs. The single CF modified with NiO NFs and corresponding local magnification images are shown in Fig. 1b. As you can see from the pictures, uniform and density 3D NiO NFs lamella were successfully grown on CFN, and such a structure with high specific surface area is benefit for following decoration. Figure 1c and insert present CdS QDs/NiO NFs/CFN. After compounding with CdS QDs, the roughness of the NiO NFs was increased which demonstrated that the CdS QDs were successfully bound to NiO NFs via coordination. The corresponding CdS QDs were characterized by transmission electron microscopy (TEM), and the result is given in Fig. S1; the synthesized CdS QDs distributed dispersedly and uniformly with diameter of particles size at ca. 5 nm. In general, the fabricated 3D hierarchical CdS/NiO heterojunction possesses large specific surface area, and that means it has more reactive sites to attach the enzymes or other biomolecules. Moreover, the hierarchical CdS/NiO heterojunction provides a shorter electron transport path which significantly enhances the photocurrent responses and is suitable for the self-powered photocathodic biosensor. To further proof the successful preparation of the CdS QDs/NiO NFs/CFN, the electrode was characterized by energy-dispersive X-ray (EDX) spectroscopy and the result is shown in Fig. S2. It showed that the Cd, Ni, O, and S elements had an even distribution on the obtained CdS QDs/NiO NFs/CFN in line with our expectations.

For exploring the distribution of elements on the CdS QDs/NiO NFs/CFN electrode at a deeper level, the X-ray photoelectron spectrum (XPS) spectra and the high-resolution XPS spectra of each element are given in Fig. 2. The three curves in Fig. 2a represent the full spectrum of bare CFN (curve black), NiO NFs/CFN (curve blue), and CdS QDs/NiO NFs/CFN (curve red), respectively. Compared to the bare CFN, NiO NFs/CFN showed the characteristic peaks of Ni 2p and O 1s, and then CdS QDs/NiO NFs/CFN had more characteristic peaks of Cd (including Cd 3d, Cd 3p, and Cd 4d) and S 2p than NiO NFs/CFN. In detail, Fig. 2b to Fig. 2f record the high-resolution XPS spectra of C 1s, O 1s, S 2p, Cd 3d, and Ni 2p. Figure 2b records the peak for C 1s at above 284 eV, which could be corresponded to the carbon in CFN. The spectrum of O 1s shown in Fig. 2c consists of two peaks at ca. 529 eV and 532 eV, which represent the lattice oxygen of the NiO crystals and the bulk O of something attached to the surface of electrode such as OH. Figure 2d presents the binding energy of S 2p located at ca. 161 eV and 162 eV which were deemed as S $2p_{3/2}$ and S $2p_{1/2}$. Figure 2e reveals two strong peaks at ca.404 eV and 411 eV which belonged to Cd $3d_{5/2}$ and Cd $3d_{3/2}$. Figure 2f shows several peaks in the range from 852 to 882 eV belonging to Ni 2p, respectively. The peaks at ca.853 eV, 855 eV, and 861 eV pertained to Ni $2p_{3/2}$ and the peaks at ca. 873 eV and 880 eV corresponded to Ni $2p_{1/2}$. These indicated the successfully fabricated of the

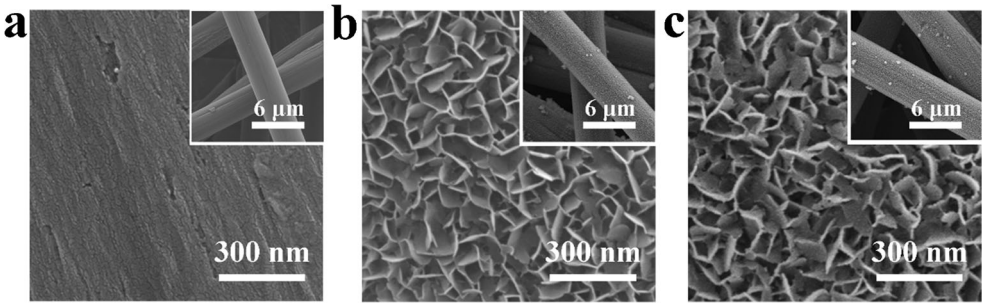

Fig. 1 Locally amplified SEM images of bare CFN (**a**), NiO NFs/CFN (**b**), and CdS QDs/NiO NFs/CFN (**c**). Inset: the corresponding images of single carbon fiber

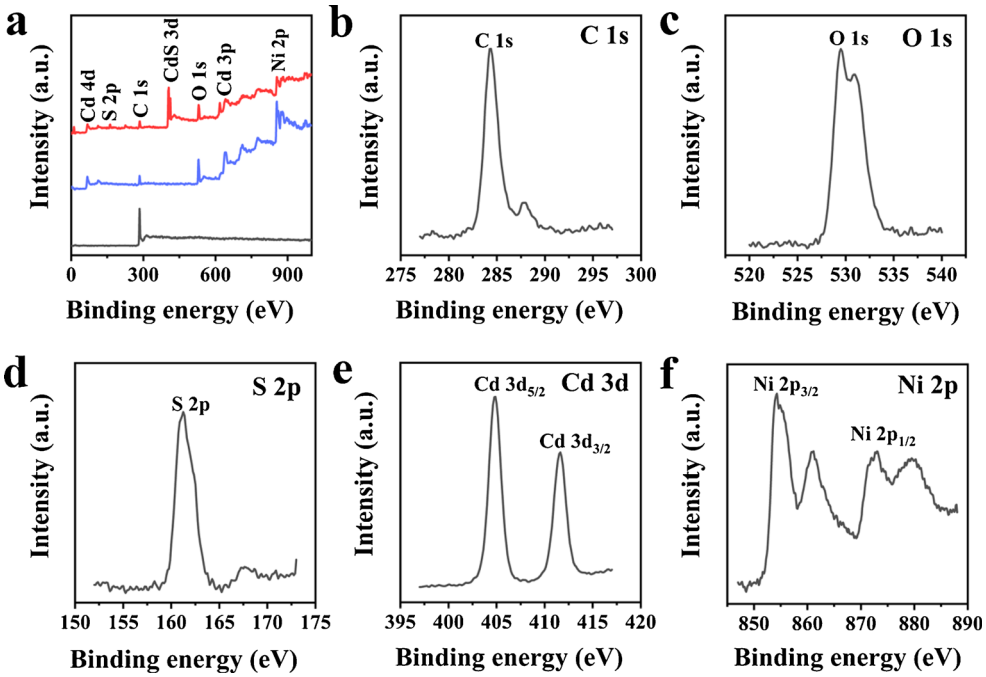

Fig. 2 XPS spectra of pristine CFN (curve black), NiO NFs/CFN (curve bule), and CdS QDs/NiO NFs/CFN (curve red) (**a**) and the high-resolution XPS spectra of C 1s (**b**), O 1s (**c**), S 2p (**d**), Cd 3d (**e**), and Ni 2p (**f**) corresponding to curve red in **a**

3D CdS QDs/NiO NFs/CFN electrode. To further confirmed the optical properties of the electrode, UV-vis characterization was performed and is illustrated in Fig. S3. As can be seen, the absorption of NiO in the visible light range is significantly lower than the CdS/NiO heterojunction. Therefore, after formation of CdS/NiO heterojunction, the photocurrent intensity in the visible light region is also enhanced as shown in Fig. 3a.

Bioanalysis application

To study the PEC property, a series of electrochemical tests on the electrode is illustrated in Fig. 3. All the experiments were conducted in 0.1 M Tris-HCl solution (pH 7.0) and 5 W 410 nm LED light without impressed voltage. The change of the photocurrent response along with the fabricated of electrode and the corresponding response to the target is demonstrated in Fig. 3a. In the beginning, pristine CFN shown barely responsive to the 410 nm excitation light (I). After deposited with NiO NFs, the photocurrent response had a slight enhancement (II). It could be attributed to that NiO was a large band gap p-type semiconductor and had weak absorption in the region of visible light. To optimize the absorption of NiO NFs/CFN electrode in visible light range, CdS QDs were chosen to combine with it because CdS has a just right narrow band gap. Then, the obtained CdS QDs/NiO NFs heterojunction will enhance the absorption notably, and increase the photocurrent intensity a lot. Furthermore, the CdS QDs/NiO NFs/CFN was conjugated with the GOx through the EDC-NHS reaction, followed by treated with 1×10^{-7} M glucose, the photocurrent signal shown significant reduction (IV). Because the process of GOx oxidized glucose would consume the dissolved oxygen in the solution which resulted in lessened of the electron acceptors and reduced the photocurrent response. The degree to which electron receptors are

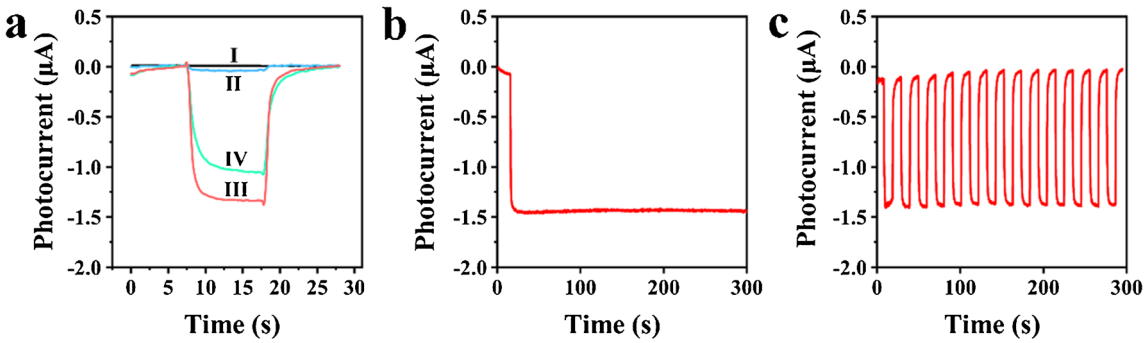

Fig. 3 Photocurrent responses of pristine CFN (I), NiO NFs/CFN (II), CdS QDs/NiO NFs/CFN (III), and GOx/CdS QDs/NiO NFs/CFN (IV) corresponding to 1×10^{-7} M glucose (**a**). The operational stability during repetitive on/off illumination cycles and the time-based photocurrent response of the CdS QDs/NiO NFs/CFN (**b**, **c**)

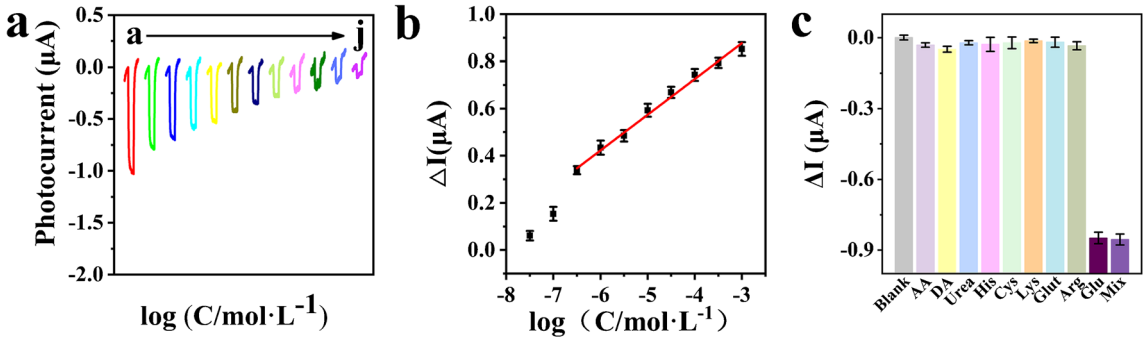

Fig. 4 Photocurrent variation corresponding to different concentration of glucose (a to j: 5×10^{-8} M, 1×10^{-7} M, 5×10^{-7} M, 1×10^{-6} M, 5×10^{-6} M, 1×10^{-5} M, 5×10^{-5} M, 1×10^{-4} M, 5×10^{-4} M, 1×10^{-3} M) (**a**) and its corresponding calibration plots (**b**). Selectivity of the fabricated CdS QDs/NiO NFs/CFN for different substance (1×10^{-3} M): blank, AA, DA, urea, His, Cys, Lys, Glut, Arg, glucose, and mixture of these (**c**)

consumed in the solution depends on the glucose concentration, the dissolved oxygen in the solution is gradually consumed as the concentration of glucose increases, and there are fewer electron receptors in the solution, resulting in a lower photocurrent.

$$C_6H_{12}O_6 + O_2 \rightarrow C_6H_{10}O_6\ (GDL) + H_2O_2$$

Figure 3b and Fig. 3c exhibit the work stability of the obtained CdS QDs/NiO NFs/CFN electrode by recording the photocurrent signal through chronoamperometric i-t curves under repetitive on/off illumination cycles and continuous illumination, respectively. Both of these pictures shown high and stable photocurrent responses under 300 s on-going detection, which proved that the CdS QDs/NiO NFs/CFN electrode was suitable for the self-powered photocathodic biosensor.

In order to verify the biosensor performance of the protocol we designed, different concentrations of glucose were detected by the GOx/CdS QDs/NiO NFs/CFN electrode. As shown in Fig. 4a, the photocurrent intensity was suppressed gradually while the glucose concentration increased. Figure 4b further demonstrates that the photocurrent response showed good linear variation corresponding to the target concentration range from 5×10^{-7} M to 1×10^{-3} M, the provided equation is $y=0.15165x + 1.33206$ ($R^2 = 0.9937$). The limit of detection was obtained at ca. 1.77×10^{-9} M through experiment which was comparable with previous reports given in Table 1.

Table 1 Comparison of proposed method with other reported assays

Method	Linear region (M)	LOD (M)	Refs
PEC	1×10^{-7}–5×10^{-3}	3.5×10^{-8}	[39]
PEC	5×10^{-6}–1×10^{-2}	1.6×10^{-6}	[40]
Photoluminescence	2×10^{-5}–2×10^{-2}	6.9×10^{-6}	[41]
Electrochemiluminescence	5×10^{-7}–8×10^{-3}	5×10^{-8}	[42]
Electrochemistry	1×10^{-3}–1.5×10^{-2}	3.9×10^{-5}	[43]
PEC	5×10^{-8}–1×10^{-3}	1.77×10^{-9}	This work

The superior analysis performance can be interpreted from the following perspectives. Firstly, to overcome the shortcoming of weak adsorption in visible light range of NiO, CdS QDs were chosen as sensitizing element. After being combined with CdS QDs, the formed hierarchical CdS/NiO heterojunction performed higher and wider adsorption in visible light range and significantly enhanced electron transfer efficiency. Secondly, upon irradiation, quick excitation, separation, and transfer of light-generated electron would occur in this system. To be specific, the photo-induced electrons could rapidly transfer from the CB of CdS QDs to the dissolved oxygen in the electrolyte which act as an electron acceptor. Meanwhile, the photo-induced holes transfer from the VB of the CdS QDs to the VB of NiO after that captured by CNF electrode to produce cathodic photocurrent responses. Finally, GOx was further combined onto the electrode. When the glucose is present, the dissolved oxygen in electrolyte would be rapidly consumed by the enzymatic catalysis and then lead to decreasing of photocurrent intensity.

To discuss the selectivity, ascorbic acid (AA), dopamine (DA), urea, histidine (His), cysteine (Cys), lysine (Lys), glutamic acid (Glut), and arginine (Arg) were selected as the interference. As shown in Fig. 4c, all the interferences were used in high concentrations and when the interferences existed apart the photocurrent variations almost no change, while the target glucose and mixture of these shown good inhibitory effect. The phenomena demonstrated that the protocol has great potential for developing sensitive self-powered PEC enzymatic biosensors.

The feasibility of the designed protocol for practical application was confirmed by a recovery experiment conducted in the fetal calf serum of glucose additions. The sample was diluted to one-twenty by 0.1 M Tris-HCl (pH 7.0). Then, added 10 μL FBS into 7 mL 0.1 M Tris-HCl buffer (pH 7.0) and measured the base value. Subsequently, added 10 μL different concentration glucose and tested the total value. The recoveries of 1×10^{-5} M, 1×10^{-4} M, and 1×10^{-3} M glucose are shown in Table S1, and the relative standard deviation (RSD) were no larger than 4.9%, which proved the

feasibility of this protocol for glucose detection in complex environment.

Conclusion

This work presented a new 3D hierarchical CdS/NiO heterojunction for high-performance self-powered photocathodic bioanalysis. The CdS QDs and NiO NFs were successfully coupled by a series of characterization and demonstrated satisfactory properties. The hierarchical CdS/NiO heterojunction was used as a glucose detection model by combined with GOx, which performed excellent analytical performances including ultra-sensitivity, high selectivity, superior stability, and application in complex sample detection. We expect the high-performance hierarchical CdS QDs/NiO NFs heterojunction could stimulate more interest in exploring novel heterostructures and spur the prosperous of self-powered photoelectrochemical biosensor. Regrettably, this method also has some limitations, for example, the preparation cycle of the electrode is time-consuming and enzyme-based sensor is prone to deactivation of enzymes.

Supplementary Information The online version contains supplementary material available at https://doi.org/10.1007/s00604-021-04882-2.

Author contribution Hui-Yu Zou: Methodology, data curation, formal analysis, validation, writing — original draft. Fen-Ying Kong: Conceptualization, methodology, data curation, formal analysis, validation, writing — original draft, funding acquisition, project administration. Xin-Yang Lu: Methodology, data curation, formal analysis, validation, writing — original draft. Meng-Jiao Lu: Methodology, data curation, formal analysis, validation, writing — original draft. Yuan-Cheng Zhu: Writing — review and editing. Rui Ban: Writing — review and editing. Wei Wang: Writing — review and editing, funding acquisition, project administration. Wei-Wei Zhao: Writing — review and editing, funding acquisition, project administration.

Funding This work was supported by the National Natural Science Foundation of China (Grant nos. 21675080, 21675139, and 21876144) and the Science and Technology Project of Guizhou Province (Grant [2017]2861, [2018]1081).

Declarations

Competing interests The authors declare no competing interests.

Conflict of interest The authors declare that they have no competing of interests.

References

1. Zhu YC, Li Z, Liu XN, Fan GC, Han DM, Zhang PK, Zhao WW, Xu JJ, Chen HY (2020) Three-dimensional CdS nanosheet-enwrapped carbon fiber framework: towards split-type CuO-mediated photoelectrochemical immunoassay. Biosens Bioelectron 148:111836
2. Zhao CQ, Zhou J, Wu KW, Ding SN, Xu JJ, Chen HY (2020) Plasmonic enhanced gold nanoclusters-based photoelectrochemical biosensor for sensitive alkaline phosphatase activity. Anal Chem 92(10):6886–6892
3. Luo ZB, Zhang LJ, Zhang R, Su LS, Tang DP (2018) Near-infrared light-excited core−core−shell UCNP@Au@CdS upconversion nanospheres for ultrasensitive photoelectrochemical enzyme immunoassay. Anal Chem 90(15):9568–9575
4. Tang J, Kong B, Wang YC, Xu M, Wang YL, Wu H, Zheng GF (2013) Photoelectrochemical detection of glutathione by IrO_2-hemin-TiO_2 nanowire arrays. Nano Lett 13(11):5350–5354
5. Kang Z, Yan XQ, Wang YF, Zhao YG, Bai ZM, Liu YC, Zhao K, Cao SY, Zhang Y (2016) Self-powered photoelectrochemical biosensing platform based on Au NPs@ZnO nanorods array. Nano Res 9(2):344–352
6. Ma ZY, Ruan YF, Xu F, Zhao WW, Xu JJ, Chen HY (2016) Protein binding bends the gold nanoparticle capped DNA sequence: toward novel energy-transfer-based photoelectrochemical protein detection. Anal Chem 88(7):3864–3871
7. Lee CY, Park HS, Fontecilla Camps JC, Reisner E (2016) Photoelectrochemical H_2 evolution with a hydrogenase immobilized on a TiO_2-protected silicon electrode. Angew Chem Int Edit 55(20):5971–5974
8. Fan L, Zhao G, Shi H, Liu M, Wang Y, Ke H (2014) A femtomolar level and highly selective 17β-estradiol photoelectrochemical aptasensor applied in environmental water samples analysis. Environ Sci Technol 48(10):5754–5761
9. Kong BA, Sikdar D, Tang J, Liu Y, Premaratne M, Zhang W, Jing YK, Zheng GF (2015) Interfacial assembly of mesoporous nanopyramids as ultrasensitive cellular interfaces featuring efficient direct electrochemistry. NPG Asia Mater 7(204):8
10. Zhao WW, Xu JJ, Chen HY (2016) Photoelectrochemical detection of metal ions. Analyst 141:4262–4271
11. Fan GC, Shi XM, Zhang JR, Zhu JJ (2016) Cathode photoelectrochemical immunosensing platform integrating photocathode with photoanode. Anal Chem 88(21):10352–10356
12. Yan K, Liu Y, Yang YH, Zhang JD (2015) A cathodic "signal-off" photoelectrochemical aptasensor for ultrasensitive and selective detection of oxytetracycline. Anal Chem 87(24):12215–12220
13. Yan K, Yang YH, Okoth OK, Cheng L, Zhang JD (2016) Visible-light induced self-powered sensing platform based on a photofuel cell. Anal Chem 88(12):6140–6144
14. Xu YT, Yu SY, Zhu YC, Fan GC, Han DM, Qu P, Zhao WW (2019) Cathodic photoelectrochemical bioanalysis. Trends Anal Chem 114:81–88
15. Kong FY, Zou HY, Xiong M, Zhang JD, Wang W, Zhao WW (2021) 3D NiO nanoflakes/carbon fiber meshwork: facile preparation and utilization as general platform for photocathodic bioanalysis. Anal Chim Acta 1143:173–180
16. Zhang L, Shi XM, Xu YT, Fan GC, Liang YY, Wang CS, Zhao WW (2019) Gold nanoparticle-induced photocurrent quenching and recovery of polymer dots: toward signal-on energy-transfer-based photocathodic bioanalysis of telomerase activity in cell extracts. Anal Chem 91(10):6403–6407
17. Jiang XY, Zhang L, Liu YL, Yu XD, Liang YY, Qu P, Zhao WW, Xu JJ, Chen HY (2018) Hierarchical $CuInS_2$-based heterostructure: application for photocathodic bioanalysis of sarcosine. Biosens Bioelectron 107:230–236
18. Dai WX, Zhang L, Zhao WW, Yu XD, Xu JJ, Chen HY (2017) Hybrid PbS quantum dots/nanoporous NiO films nanostructure: preparation, characterization, and application for novel self-powered cathodic photoelectrochemical biosensor. Anal Chem 89(15):8070–8078

19. Zhou Y, Shi Y, Wang FB, Xia XH (2019) Oriented self-assembled monolayer of Zn(ii)-tetraphenylporphyrin on TiO_2 electrode for photoelectrochemical analysis. Anal Chem 91(4):2759–2767
20. Zhang BH, Wang H, Xi JJ, Zhao FQ, Zeng BZ (2020) Novel $Bi_{2+x}WO_6$ p-n homojunction nanostructure: preparation, characterization, and application for a self-powered cathodic photoelectrochemical immunosensor. ACS Sens 5(9):2876–2884
21. Yu SY, Zhang L, Zhu LB, Gao Y, Fan GC, Han DM, Chen GX, Zhao WW (2019) Bismuth-containing semiconductors for photoelectrochemical sensing and biosensing. Coord Chem Rev 393:9–20
22. Cai GN, Yu ZZ, Tang DP (2020) Actuating photoelectrochemical sensing sensitivity coupling core-core-shell Fe_3O_4@C@TiO_2 with molecularly imprinted polypyrrole. Talanta 219:121341
23. Long D, Li M, Wang H, Chai Y, Li Z, Yuan R (2020) Ultrasensitive photoelectrochemical assay for DNA detection based on a novel SnS_2/CO_3O_4 sensitized structure. Anal Chem 92(21):14769–14774
24. Meng LX, Xiao K, Zhang XH, Du CC, Chen JH (2020) A novel signal-off photoelectrochemical biosensor for M.SssI MTase activity assay based on GQDs@ZIF-8 polyhedra as signal quencher. Biosens Bioelectron 150:111861
25. Pang XH, Cui C, Su MH, Wang YG, Wei Q, Tan WH (2018) Construction of self-powered cytosensing device based on ZnO nanodisks@g-C_3N_4 quantum dots and application in the detection of CCRF-CEM cells. Nano Energy 46:101–109
26. Meng LX, Xiao K, Zhang XH, Du CC, Chen JH (2020) DNA-linked CdSe QDs/AGQDs "Z-scheme" system: ultrasensitive and highly selective photoelectrochemical sensing platform with negative background signal. Sensors Actuators B Chem 305:127480
27. Jia YM, Wu F, Liu PL, Zhou GH, Yu B, Lou XD, Xia F (2019) A label-free fluorescent aptasensor for the detection of Aflatoxin B1 in food samples using AIEgens and graphene oxide. Talanta 198:71–77
28. Han YJ, Zhu ZJ, Huang L, Guo YJ, Zhai YL, Dong SJ (2019) Hydrothermal synthesis of polydopamine-functionalized cobalt-doped lanthanum nickelate perovskite nanorods for efficient water oxidation in alkaline solution. Nanoscale 11:19579–19585
29. Shi Y, Zhang Q, Zhai TT, Zhou Y, Yang DR, Wang FB, Xia XH (2018) Localized surface plasmon resonance enhanced label-free photoelectrochemical immunoassay by Au-MoS_2 nanohybrid. Electrochim Acta 271:361–369
30. Wang Y, Liu Q, Wei J, Dai Z, Ding L, Yuan R, Wen Z, Wang K (2020) Visible light-driven photoelectrochemical ampicillin aptasensor based on an artificial Z-scheme constructed from $Ru(bpy)_3^{2+}$-sensitized BiOI microspheres. Biosens Bioelectron 173:112771
31. Peng B, Lu Y, Luo J, Zhang ZL, Zhu X, Tang L, Wang LL, Deng YC, XL OY, Tan JS, Wang JJ (2020) Visible light-activated self-powered photoelectrochemical aptasensor for ultrasensitive chloramphenicol detection based on DFT-proved Z-scheme Ag_2CrO_4/g-C_3N_4/graphene oxide. J Hazard Mater 401:123395
32. Zhang Z, Zhang M, Xu Y, Wen Z, Ding C, Guo Y, Hao N, Wang K (2020) Bi^{3+} engineered black anatase titania coupled with graphene for effective tobramycin photoelectrochemical detection. Sensors Actuators B Chem 321:128464
33. Galant AL, Kaufman RC, Wilson JD (2015) Glucose: detection and analysis. Food Chem 188:149–160
34. Dai J, Wu Y, Chen SW, Zhu S, Yin HP, Wang M, Tang J (2010) Sugar compositional determination of polysaccharides from Dunaliella salina by modified RP-HPLC method of precolumn derivatization with 1-phenyl-3-methyl-5-pyrazolone. Carbohydr Polym 82(3):629–635
35. Park S, Chung TD, Kim HC (2003) Nonenzymatic glucose detection using mesoporous platinum. Anal Chem 75(13):3046–3049
36. Carballo S, Zingarello FA, Maestre SE, Todolí JL, Prats MS (2014) Optimisation of analytical methods for the characterisation of oranges, clementines and citrus hybrids cultivated in S pain on the basis of their composition in ascorbic acid, citric acid and major sugars. Int J Food Sci Technol 49(1):146–152
37. Dong XC, Xu H, Wang XW, Huang YX, Chan-Park MB, Zhang H, Chen P (2012) 3D graphene–cobalt oxide electrode for high-performance supercapacitor and enzymeless glucose detection. ACS Nano 6(4):3206–3213
38. Zhao WW, Chen R, Dai PP, Li XL, Xu JJ, Chen HY (2014) A general strategy for photoelectrochemical immunoassay using an enzyme label combined with a CdS quantum dot/TiO_2 nanoparticle composite electrode. Anal Chem 86(23):11513–11516
39. Zhen S, Fan GC, Li ZM, Gao FX, Luo XL (2018) Universal design of selectivity-enhanced photoelectrochemical enzyme sensor: integrating photoanode with biocathode. Anal Chem 90(18):10681–10687
40. Zhang L, Ruan YF, Liang YY, Zhao WW, Yu XD, Xu JJ, Chen HY (2018) Bismuth oxyiodide couples with glucose oxidase: a special synergized dual-catalysis mechanism for photoelectrochemical enzymatic bioanalysis. ACS Appl Mater Interfaces 10(4):3372–3379
41. Ghosh J, Ghosh R, Giri PK (2018) Tuning the visible photoluminescence in Al doped ZnO thin film and its application in label-free glucose detection. Sensors Actuators B Chem 254:681–689
42. Jiang JJ, Chen D, Du XZ (2017) Ratiometric electrochemiluminescence sensing platform for sensitive glucose detection based on in situ generation and conversion of coreactants. Sensors Actuators B Chem 251:256–263
43. Xu XC, Niu XH, Wu SW, Zou XB, Pan JM (2018) A detachable and recyclable electrochemical sensor for high-performance detection of glucose based on boronate affinity. Sensors Actuators B Chem 268:430–437

Publisher's note Springer Nature remains neutral with regard to jurisdictional claims in published maps and institutional affiliations.